Signal Processing and Renewable Energy
June 2019, (pp. 9-24)
ISSN: 2588-7327
eISSN: 2588-7335

A Comparative Study on Despeckling Techniques in Intravascular Ultrasound Images

Sima Navabian[1], Fereshteh Yousefi Rizi[1*], Zahra Alizadeh Sani[2]

[1] Bioelectric Department, Biomedical Engineering Faculty, South Tehran Branch, Islamic Azad University, Tehran, Iran.
[2] Department of Rajaie Cardiovascular Medical and Research Center, Iran University of Medical Sciences, Tehran, Iran.

Received:27-Oct-2018, Revised: 18-Dec-2018, Accepted: 01-Jan-2019.

Abstract

Intravascular ultrasound (IVUS) imaging is a diagnostic imaging technique for tomographic visualization of coronary arteries and studying atherosclerotic diseases. These medical images are generally corrupted by multiplicative speckle noise due to the interference of the signal with the backscattered echoes. Speckle noise is an inherent property of medical ultrasound imaging, and it generally tends to reduce the image quality; thus, removing noise from the original medical image is a challenging problem for diagnosis applications. Trying to reduce speckle assists experts for better understanding of some pathologies and diagnosis purposes. Recently, several techniques have been proposed for effective suppression of speckle noise in ultrasound B-Scan images. In this paper, we overview the denoising techniques in both spatial and transform domain, and propose a new despeckling method based on Shearlet transform and ant colony optimization. To quantify the performance improvements of the speckle noise reduction methods, various evaluation criteria in addition to the visual quality of the denoised images are used. Our results showed that in general Shearlet transform with three different types of threshold selection is faster and more efficient than other techniques. In the case of accurate estimation of the variance of noise, Shearlet transform based on ACO yields acceptable results in comparison with others methods. This technique can obtain a favorable signal-to-noise ratio and successfully improve the quality of images and preserve edges and curves as well.

Keywords: Ant Colony, Curvelet, Contourlet, Despeckling, Dual-tree Complex Wavelet (DT-CWT), Intravascular Ultrasound (IVUS) Imaging, Shearlet.

1. INTRODUCTION

Since the birth of computer science, medical imaging devices such as X-ray, CT, MRI, and ultrasound have been a great help for

*Corresponding Author's Email: f_yousefirizi@azad.ac.ir

medicine in general. They show the new information about the inside of the human body. Among these imaging techniques, ultrasound imaging is popular as a noninvasive, low cost, and portable real time imaging [1], [2].

Intravascular ultrasound (IVUS) imaging is a new modality, works based on the inserted catheter directly into the blood vessel that provides the real-time cross-sectional view of the vessel wall. This technique provides the quantitative assessment of the lumen structure that cannot be visualized by an angiography [3]. IVUS images are generally corrupted by a kind of multiplicative noise called speckle, which is the result of the constructive and destructive coherent summation of ultrasound echoes that degrades the fine details, edge definitions and limit the contrast resolution by making it difficult to detect small and low contrast lesions in body. Therefore, despeckling of medical ultrasound images is a critical pre-processing step for better diagnosis of some pathologies and in order to investigate the various vessel wall diseases [4],[5].

Various techniques have been proposed to remove the linear and nonlinear noise from an image in order to increase the image quality [6], [7]. Most widely different types of filters are used for speckle noise reduction in ultrasound images. For instance, Mean filter is the least satisfactory method of speckle noise reduction as it results in loss of detail and decrease the image resolution by blurring effect [8]. Median filter is used for despeckling due to its robustness against impulsive noise and edge preserving characteristic. This type of filter produces less blurred images than Mean filter but the disadvantage is time consuming. As this filter should find the median, it is necessary to sort all the value in the neighborhood into numerical order. So, because of an extra computation time is needed to sort the intensity value of each set [9], median filter is time consuming. Wiener filter provides better result in noise reduction, it preserves edges and other high frequency information of the image but requires more computation time and also this type of filter is basically designed for additive noise suppression [10]. To overcome this issue, Jain [11] developed a homomorphic filter where the multiplicative speckle noise is converted into additive noise by using the logarithm of input image. Non-linear estimator such as Bayesian was also developed for noise reduction with outperform classical linear methods [12]. Another denoising techniques such as Multiresolution Bio Lateral Filtering [13], Total Variations [14] and Kernel Regression [15] have been proposed in the past decades, all of these methods estimated the denoised value pixel based on the information provided in a surrounding local limited window, but Buades developed a more efficient algorithm called Non-local Means Algorithm (NLM) based on averaging similar patches in image which exhibits capability to preserve fine details [16].

Over the last decades, there has been abundant interest in Wavelet based method noise reductions in signals and images. Wavelet transforms can achieve the good denoising result but they can capture only limited directional information [17]. Although Wavelets have been extensively

used in speckle noise reduction, it has been shown [18] that speckle denoising using Contourlet provides better results in comparison with Wavelet Shirinkage and Dual-tree Wavelet transform. As Wavelet is generally the optimal base, when it represents the objective function with point singularity, but it is not the optimal method when it represents the singularity of line or hyper plane. To overcome the exciting drawback of the classical multiresolution approaches such as Wavelets, a kind of multiscale transform based on Ridgelet transform called Curvelet, has rapidly developed by Cande's and Donoho [19]. This transform can detect the singularity of line and surface in two dimensional (2-D) spaces. Recently, a new denoising method for images based on Shearlet transform has been carried out [20], [21]. In this paper, we present a comparative study of the performance of various despeckling techniques which are widely used for ultrasound images.

This paper is organized as follows: Section 2 describes despeckling methods in both spatial domain and transform domain used in this paper. Section 3 presents the experimental results and gives the used data in this paper. Finally Section 4 concluds the paper.

2. PROBLEM FORMILATION

Over the years, several techniques have been proposed to reduce the effect of speckle noise within ultrasound images. Among these methods, we consider a number of techniques which is extensively used in both spatial and transform domain, to despeckle the ultrasound images.

2.1. Spatial Domain

Spatial filtering is a traditional technique to remove noise from the image. In spatial domain, the filtering is based on statistical relationship between the center pixel and surrounding pixels, a window known as a mask (kernel) moved over each pixel of the image and the value of the current pixel is being replaced by the other pixels in the neighborhood, and this procedure continue until the entire image is being covered.

They are different types of filters in this field, which is commonly used for speckle noise reduction, some well-known methods are listed in following.

- **Median filter:** it is a spatial nonlinear filter [9] which works according to compute the median of all pixels within the local window. This type of filter produces less blurred images in compare with mean filter, but the disadvantage of this method is the extra computation time needed to sort the intensity value of each set.
- **Lee filter:** Lee filter is one of the earliest filters that working directly on the intensity of the image using local statics and it can effectively preserve edges and features [22]. Lee filtering technique is based on the approach that if the variance over an area is low or constant then the smoothing will not be performed. Conteraversa, if the variance over an area is high then the smoothing is to be done,

$$Img(i.j) = im + W * (C_p - Im) \qquad (1)$$

where Img is pixel value at indices $(i.j)$ after filtering, Im is the image mean

intensity, C_p is the center pixel and W is the filter window. The major disadvantage of Lee filter is, it ignores the fact that speckle noise is existed in the areas closest to edges and lines.

- **Wiener filter:** The wiener filter is also known as a least mean square filter. It performs the image smoothing based on the computation of local image variance. If the image variance is large, the smoothing is ignorable and vice versa. It has capacity to restore images even if they are corrupted or blurred [10].
  Wiener filtering is given by,

$$f(u.v) = \frac{H(u.v)^*}{H(u.v)^2 + \left[\frac{Sn\,(u.v)}{Sf\,(u.v)}\right] G(u.v)} \quad (2)$$

  where $H(u.v)$ is degradation function, $G(u.v)$ is degraded image, $Sn\,(u.v)$ is the power spectra of noise and $Sf\,(u.v)$ is the power spectra of original image. Wiener filter provides better result in noise reduction, it preserves edges and other high frequency information of the image than the linear filtering but requires more computation time and also this type of filter is basically designed for additive noise suppression.

- **Non-local Means Algorithm (NLM)**
  In recent years, patch-based image denoising algorithms like Non-local Means filter which proposed by Buades [16] have gotten much more attention to deal with denoising problems. Most of denoising techniques degrade or remove the fine details and texture, but non-local means filtering decreases the loss of fine image details and also improve the peak signal to noise ratio. This filtering technique is based on a non-local averaging of all pixels in the image and unlike local means filter which takes the mean value of pixels surrounding the target pixel to smooth the image, non-local means algorithm takes a mean of all pixels in the image weighted by the similarity between the local neighborhood of the pixel being processed and local neighborhood of surrounding pixels.

  The estimated pixel value 'p' using NLM algorithm is computed as a weighted average of all the pixels in the image as,

$$NL(V)(p) = \sum_{q \in v} W(p.q)\, V(q) \quad (3)$$

  where V is the noisy image, and weights $W(p.q)$ satisfy the following condition $0 \le W(p.q) \le 1$ and $\sum_{q \in v} W(p.q) = 1$.

  Although NLM method can achieve appropriate PSNR, there are still several issues which can reduce the algorithm efficiency. In particular, the performance of NLM depends on the proper selection of the internal parameters such as patch size, and search region size [16].

2.2. Transform Domain

Transform domain techniques has got wide spread applications in the field of denoising where the image is transformed into frequency domain. The basic assumption is that the transform domain contains the basic elements in different shapes and directions

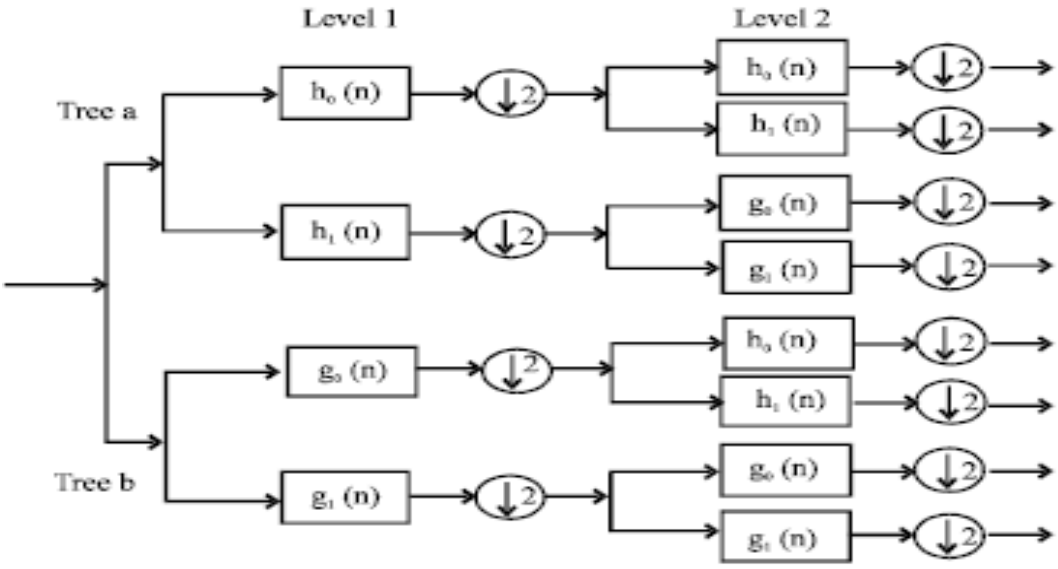

Fig. 1. Dual-tree complex wavelet transform filter bank [17].

[23]. Despeckling techniques in frequency domain consist of calculating the transform domain coefficients and carrying out filtering of these coefficients based on the threshold value.

The well-known transform domain techniques include Wavelet (Dual-tree Complex Wavelet Transform), Contourlet, Curvelet and Shearlet, which are explained in following [17, 18, 19, 20].

2.2.1. Wavelet Transform

Wavelet techniques are successfully applied to various problems in image processing. Although the Discrete Wavelet Transform (DWT) has led to many applications but it has been suffered from two main disadvantages [17]:

1. Lack of shift invariance, which means that small shift in the input signal can cause major variations in the distribution of energy among DWT coefficients at different scales.
2. Poor directional selectivity due to the separable and real wavelet filters characteristics.

To overcome this limitation, Complex Wavelet Transform (CWT) was proposed [19]. CWT employs analytic filters having real and imaginary part which constructed from Hilbert transform. Unfortunately, CWT have not been widely used in image processing due to difficulty designing complex filters which satisfy perfect reconstruction (PR) properties.

An effective approach for implementing analytic wavelet transform introduced in 1998 and called Dual-tree Complex Wavelet Transform (DT-CWT).

The DT-CWT employs two real DWT 's that uses two different set of filters with PR satisfaction properties. The first DWT yields the real part of the transform while the second DWT gives the imaginary part. DT-CWT, as shown in Fig. 1, decompose a low-

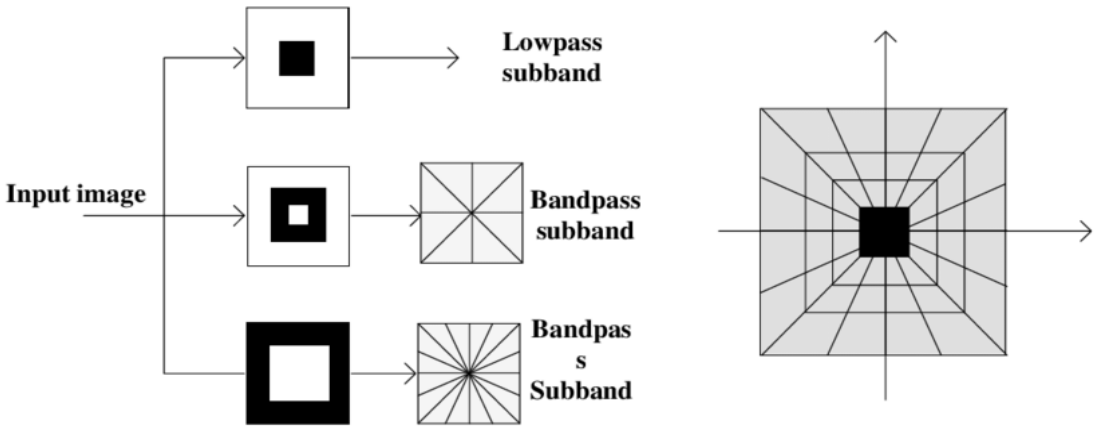

Fig. 2. Contourlet transform double filter bank [18].

resolution image into different sub-band images. A one level CWT of an image produces two complex-valued low frequency sub-band images and six complex-valued high frequency sub-band images [19].

2.2.2. Contourlet Transform

Contourlet transform proposed in 2002, is one of the recent system representations for image analysis [18]. It offers several advantages over the Wavelet transform in terms of representing geometrical smoothness more efficiently. Contourlet transform provides a high degree of the directionality, anisotropy and flexible aspect ratio. This technique employs a double filter bank structure in which at first the Laplacian Pyramid (LP) is used to capture the point of discontinuities and multiscale transform, followed by the directional filter bank (DFB) to link discontinuities to linear structures. DFB was designed to capture the high frequency components present in different directions. As the low frequency components are handled poorly, the DFB is combined with Laplacian Pyramid (LP) where the low frequency components are removed before applying directional filter bank (DFB). Owning to the geometrical information, the Contourlet transform achieves better results than DWT in image analysis applications. However due to down sampling and up sampling present in both LP and DFB stage, the Contourlet transform is not shift-invariant.

Contourlet transform decompose image into several sub-bands at multiple scale. Fig. 2 shows the block diagram for the Contourlet filter bank. First a multiscale decomposition into octave bands by LP is computed and then a directional filter bank (DFB) is applied to each band-pass channel. The multiscale representation obtained from LP structure is used as the first stage in Contourlet transform.

2.2.3. Curvelet Transform

Curvelet transform as a multiscale transform developed in 1999 in an attempt to overcome inherent limitation of traditional multiscale representation such as Wavelets

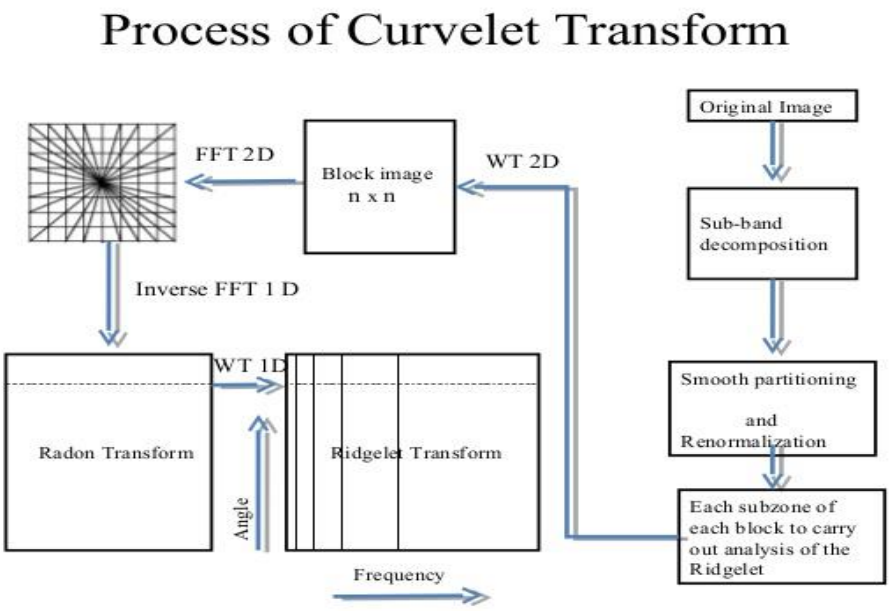

Fig. 3. Curvelet transform tilling [19].

[19]. Curvelets provide a sparse representation for images with different geometrical structures which is suitable for representing curve discontinuities. This transform has various structure elements which include the parameters of dimension, location and orientation that cause Curvelet transform became much more efficient than wavelets in the expression of image edges such as geometry characteristics of curve and beeline that has already obtained good results in image denoising. In Curvelet domain, the signal is sparse but the noise is espread. In other word, signal and noise have minimal overlap in Curvelet domain. This property makes Curvelet transform as a superior method for despeckling ultrasound images. The main advantage of methods based on Curvelet transform is the ability to use relatively small number of coefficients to reconstruct edge details at an image. Each matrix of coefficients is characterized by both angle and scale as,

$$C_{m.n}^{j.l} = < f, \Phi_{m.n}^{j.l} > \quad (4)$$

where Φ is the basis function, j and l are scale and angle respectively and m, n are an index which is limited according to j and l parameters. Full description of the Curvelet transform and it's mathematical formulation is given in [19].

2.2.4. Shearlet Transform

Shearlet transform as a non-adaptive multiscale technique developed in 2005 to overcome the limitations of Wavelet and Contourlet transform [20], [21]. Shearlets are considered as the sloping waveform with directions organized by shear parameters. It was shown that Shearlets are more efficient in compare with Wavelets to represent an

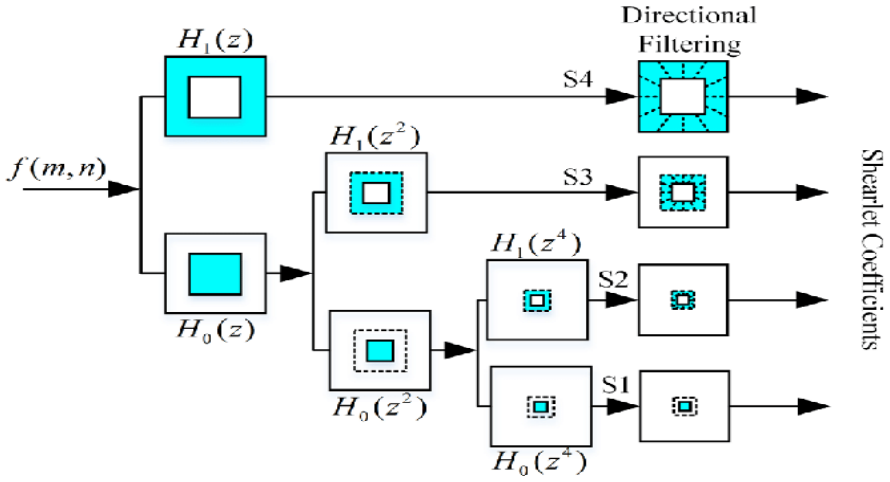

Fig. 4. filter bank structure of Shearlet transform [20].

anisotropic features such as edges. A Shearlet is generated by dilation, shearing and translation of a function ψ, called mother Shearlet,

$$\psi_{a.s.t} = a^{-\frac{3}{4}} \psi\left(A_a^{-1} S_s^{-1}(x-t)\right) \qquad (5)$$

where $t \in R^2$ is a translation, A_a is a dilation matrix and S_s is a shearing matrix defined by:

$$A_a = \begin{pmatrix} a & 0 \\ 0 & \sqrt{a} \end{pmatrix} \qquad S_s = \begin{pmatrix} 1 & -s \\ 0 & 1 \end{pmatrix} \qquad (6)$$

The anisotropic dilation A_a controls the scale of shearlets by applying the different dilation factor along two axes and the shearing matrix S_s determines the orientations of shearlets. Shearlet transform decompose the input image into a number of sub-band images containing high rate and low rate of recurrence sub-band images. The magnitude of each and every Shearlet sub-band has the same magnitude as the initial image [20]. The decomposition is highly redundant.

Fig. 4 represents a three level multiscale, shift invariant and multi directional decomposition, since it shows during the first level of decomposition it will give one approximation and n directional detailed bands, the first approximation is given for further level decomposition.

2.2.5. Proposed Method based on Shearlet and Ant Colony Optimization

As it was mentioned in the previous Section, Shearlet transform was introduced with the expressed intent to provide a highly efficient representation of images with edges which overcomes the limitation of traditional methods in order to despeckling IVUS images. Shearlet shrinkage is an image denoising technique based on the concept of thresholding the Shearlet coefficients. The key challenge of Shearlet shrinkage is to find an appropriate threshold value, which is typically controlled by the signal variance. To tackle this challenge, a new image

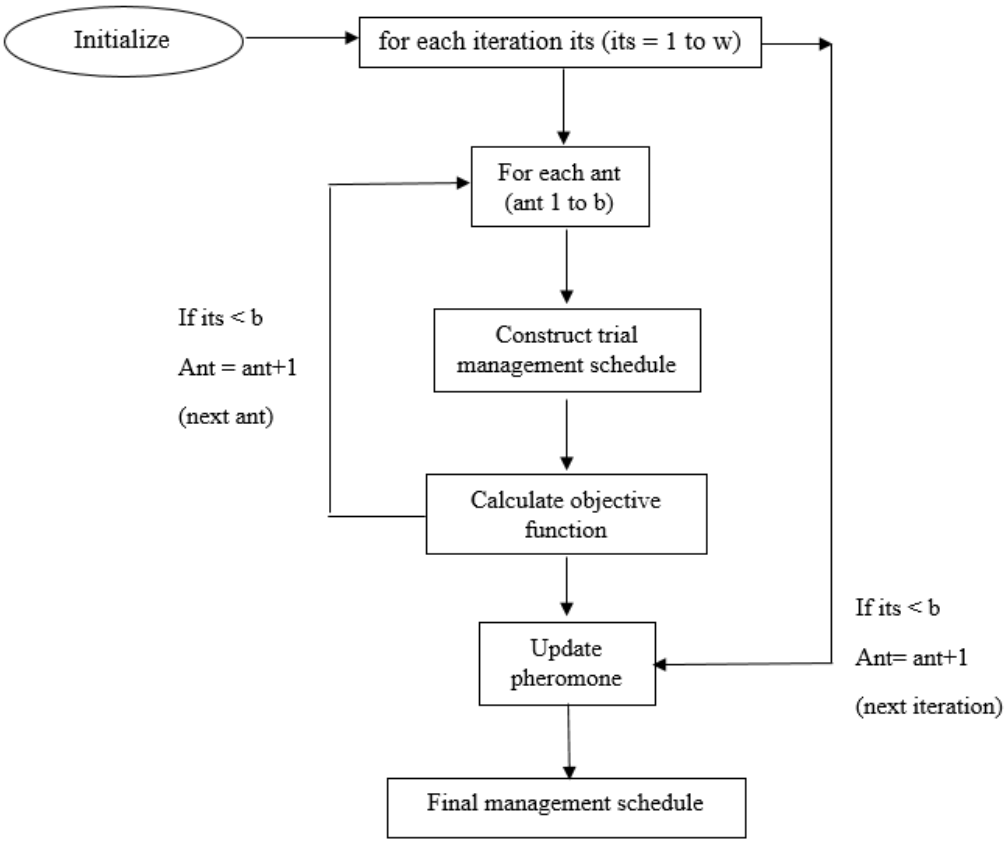

Fig. 5. ACO block diagram [25].

shrinkage approach called AntShrink is proposed in this paper.

Ant Colony Optimization (ACO) [24] is a meta-heuristic method for solving hard combinatorial optimization problems. ACO is a nature-inspired optimization algorithm motivated by the natural collective behavior of real-word ant colonies. in this paper, ACO technique is used to classify the Shearlet coefficients and denoising IVUS images.

The basic steps in ACO algorithm can be expressed as follows [25]:

1. Initialize the position of each ant, as well as the pheromone matrix τ^0.
2. For the construction-step index $n = 1{:}N$,
   - ✓ Consecutively move each ant for L steps, according to a probabilistic transition matrix $P^{(n)}$ (with a size of $M_1M_2 \times M_1M_2$).
   - ✓ Update the pheromone information matrix $\tau^{(n)}$.
3. Make the solution decision according to the final pheromone information matrix $\tau^{(N)}$.

There are two fundamental issues in the above ACO process; that is, the establishment of the probabilistic transition matrix $P^{(n)}$ and the update of the pheromone information matrix $\tau^{(N)}$, each of them is presented in detail as follow,

$$P_{i,j}^{(n)} = \frac{(\tau_{i,j}^{(n-1)})^{\alpha}(\eta_{i,j})^{\beta}}{\sum_{j\epsilon\Omega_i}(\tau_{i,j}^{(n-1)})^{\alpha}(\eta_{i,j})^{\beta}} \quad (7)$$

$$\tau_{i,j}^{(n-1)} = \begin{cases} \tau_{i,j}^{(n-1)} + \Delta_{i,j}^{(k)} & if\ (i,j)\ belongs\ to\ the\ best\ tours \\ \tau_{i,j}^{(n-1)}, & otherwise \end{cases} \quad (8)$$

A noisy image in Shearlet domain can be mathematically modeled as [25]:

$$Y = s * n \quad (9)$$

where 'Y' is the observed noisy coefficients, 's' is the unknown noise-free coefficients, and 'n' is assumed to be a noise with a zero mean and a variance σ_n^2. The goal of image denoising is to recover the signal 's' from the noisy observation 'Y'.

For better comparison, hard thresholds and shrinkage thresholds have also been investigated in this paper [27].

3. EXPERIMENTAL RESULTS

3.1. Data Base

The IVUS image data set used for the proposed method validation is given from [26]. The images, with size 500×500 pixels, were acquired using a 30-MHz transducer at a pullback speed of 0.55 m/s and a grabbing rate of 10 frames/s. This process is carried out using the ultrasound system developed by the Volcano therapeutics INC. (model Invision TM, IVG-EE).

3.2. Evaluation Criteria

Several experiments were conducted to evaluate the despeckling ultrasound images, to quantitative performance analysis.Well accepted metrics such as peak signal to noise ratio (PSNR) and mean square error (MSE) are used.

PSNR is an objective measure which evaluates the intensity changes of an image between the original and enhanced image. The formula for calculating PSNR is given bellow:

$$PSNR = 10\log 10\ (\frac{R^2}{MSE}) \quad (10)$$

Another evaluation criterion is MSE which is computed as:

$$MSE = \frac{1}{K}\sum_{i=1}^{k}(\widehat{S_i} - S_i)^2 \quad (11)$$

Note that the high-quality image has small value of PSNR and large value of MSE means that image has poor quality. Contrast-to-noise ratio (CNR) and figure of merit (FOM) are another evaluation metrics which are respectively used to determine image quality and the performance of edge preservation of the image,

$$CNR = \frac{|\mu' - \mu''|}{\sqrt{\sigma_1^2 - \sigma_2^2}} \quad (12)$$

$$FOM = \frac{1}{\max(N_e.N_i)}\sum_{j=1}^{N}\frac{1}{1+d_j^2 a} \quad (13)$$

The results of calculated evaluation criteria for denoising results are summarized in Table 1, 2 and 3.

Based on the results in Tables 1 and 2, the higher PSNR in both spatial and transform domain, is obtained by the Lee filter and Shearlet transform respectively that indicates the effectiveness of these proposed method for IVUS despeckling.

In this paper, the ACO optimization algorithm is used to find an appropriate threshold value and so denoising IVUS images. For better comparison, hard threshold and shrinkage threshold have also been investigated. The results of calculated evaluation criteria for despeckeling IVUS images are summarized in Table 3.

Based on the results in Tables 1 and 2, the higher PSNR in both spatial and transform domain, is obtained by the Lee filter and Shearlet transform respectively that indicates the effectiveness of these proposed method for IVUS despeckling.

In this paper, the ACO optimization algorithm is used to find an appropriate threshold value and so denoising IVUS images. For better comparison, hard threshold and shrinkage threshold have also been investigated. The results of calculated evaluation criteria for despeckeling IVUS images are summarized in Table 3.

According to Table 3, in general Shearlet transform based on ACO yields acceptable results in comparison with other despeckling methods.

The results of the threshold approaches show that, ACO based Shearlet yields accurate estimation of noise variance point

Table 1. ***The performance metrics results of despeckling methods in spatial domain (x: original image n: noisy version xr: denoised image).***

Noise Variance	PSNR (x,xr)	MSE (x,xr)	Spatial Domain															
			Lee Filter				Median Filter				Wiener Filter				NLM Algorithm			
			Psnr (x,xr)	Mse (x,xr)	Cnr (x,xr)	Fom (x,xr)	Psnr (x,xr)	Mse (x,xr)	Cnr (x,xr)	Fom (x,xr)	Psnr (x,xr)	Mse (x,xr)	Cnr (x,xr)	Fom (x,xr)	Psnr (x,xr)	Mse (x,xr)	Cnr (x,xr)	Fom (x,xr)
0.04	24.56	0.059	32.24	0.016	53.50	91.07	28.42	0.037	57.71	88.33	27.99	0.039	48.37	85.5	27.68	0.041	55.78	92.29
0.05	23.59	0.066	31.48	0.018	53.40	90.14	27.84	0.040	57.63	87.13	27.20	0.043	48.81	90.01	27.18	0.043	56.66	89.11
0.06	22.83	0.072	30.78	0.019	54.55	89.07	27.41	0.042	58.28	86.70	26.49	0.047	49.26	86.00	26.88	0.045	57.94	88.78

Table 2. ***The performance metrics results of despeckling methods in transform domain (x: original image n: noisy version xr: denoised image).***

Noise Variance	PSNR (x,xr)	MSE (x,xr)	Transform Domain															
			DT-CWT				Contourlet				Curvelet				Shearlet			
			Psnr (x,xr)	Mse (x,xr)	Cnr (x,xr)	Fom (x,xr)	Psnr (x,xr)	Mse (x,xr)	Cnr (x,xr)	Fom (x,xr)	Psnr (x,xr)	Mse (x,xr)	Cnr (x,xr)	Fom (x,xr)	Psnr (x,xr)	Mse (x,xr)	Cnr (x,xr)	Fom (x,xr)
0.04	24.56	0.059	27.45	0.029	52.85	79.04	30.00	0.024	53.67	88.77	30.84	0.031	51.28	88.73	32.72	0.017	54.30	92.42
0.05	23.59	0.066	27.22	0.030	53.11	81.93	29.17	0.026	54.08	90.20	29.29	0.036	51.51	88.82	32.17	0.018	53.91	90.57
0.06	22.83	0.072	26.89	0.031	53.40	80.25	29.08	0.028	54.26	89.32	28.19	0.042	51.45	88.29	31.60	0.019	54.74	89.37

Table 3. ***Performance metrics results of denoising methods in different type of Shearlet transform (x: original image n: noisy version xr: denoised image).***

Noise Variance	PSNR (x,xr)	MSE (x,xr)	Shearlet-Hard				Shearlet-Shrinkage				Shearlet-ACO			
			Psnr (x,xr)	Mse (x,xr)	Cnr (x,xr)	Fom (x,xr)	Psnr (x,xr)	Mse (x,xr)	Cnr (x,xr)	Fom (x,xr)	Psnr (x,xr)	Mse (x,xr)	Cnr (x,xr)	Fom (x,xr)
0.04	24.56	0.059	34.83	0.023	53.91	92.44	26.96	0.046	52.78	90.08	29.80	0.029	52.66	93.75
0.05	23.59	0.066	34.56	0.023	54.29	90.86	26.02	0.051	52.83	86.65	28.99	0.037	52.31	91.92
0.06	22.83	0.072	33.98	0.025	54.55	88.89	25.23	0.056	53.08	86.66	28.17	0.040	53.67	93.06

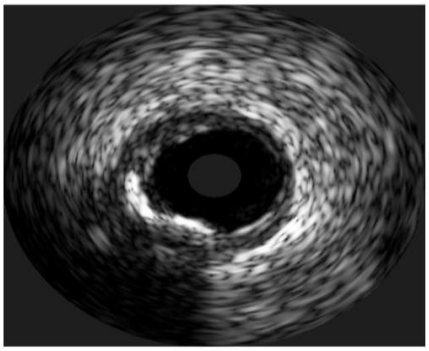

Original IVUS image

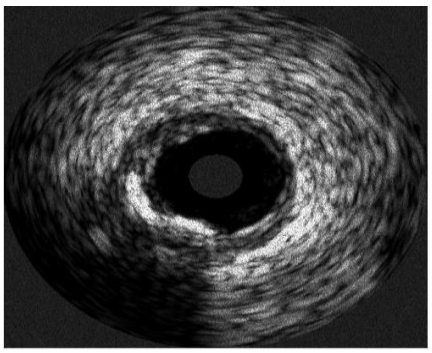

Noisy image (variance =0.06)

De-noised images

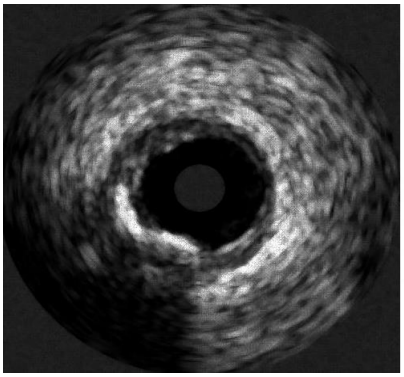

Median Filter

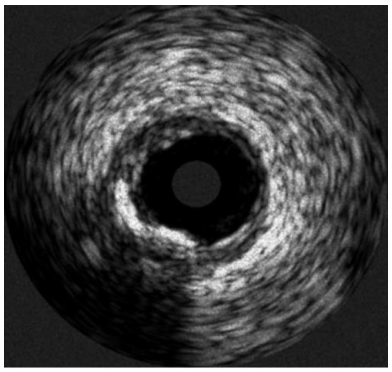

Lee Filter

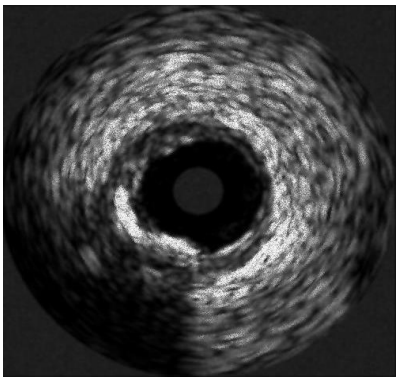

Wiener Filter

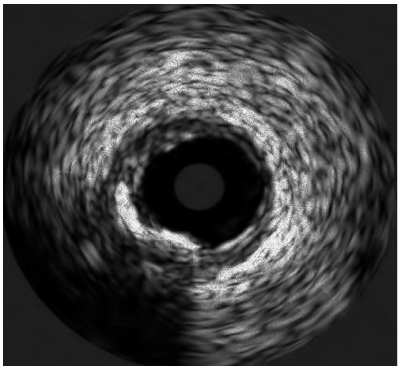

Non-Local Means Algorithm

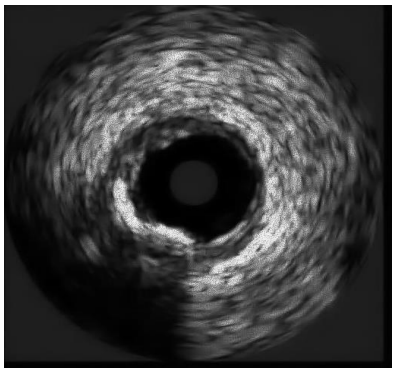

Dual-tree Wavelet

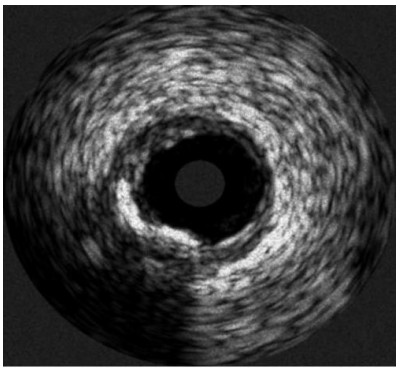

Contourlet

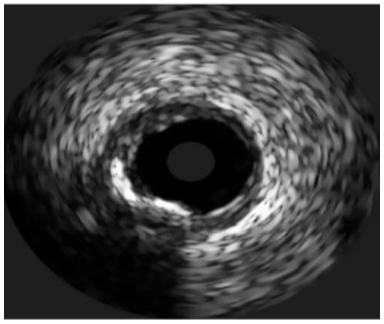

Curvelet

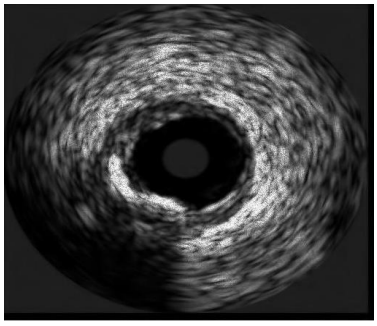

Shearlet

Continued

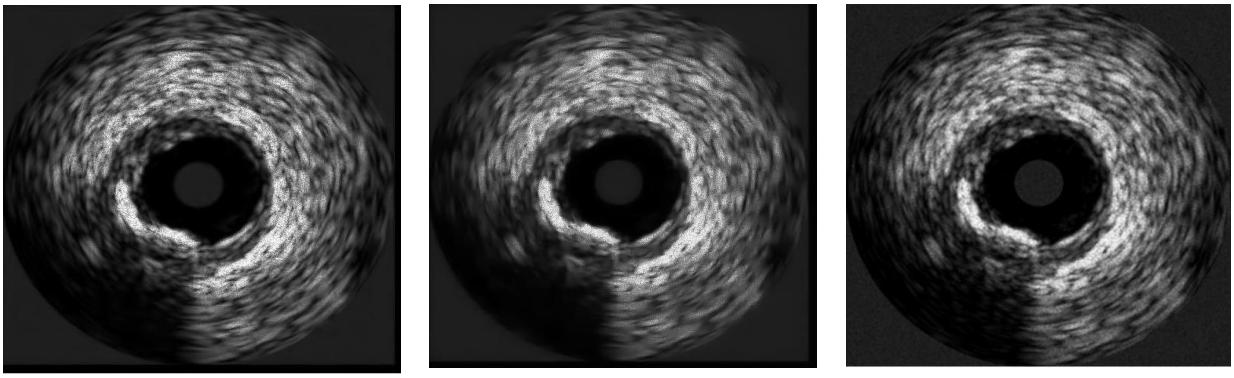

Shearlet-Hard Shearlet-Shrinkage Shearlet-ACO

Fig. 6. Qualitative result of various despeckling techniques.

of view. Shearlet based ACO obtain a favorable signal-to-noise ratio and can successfully improve the quality of images and edges and curves

In addition to this performance metric, the visual inspection of the denoised images is used. So, for better visual inspection, Fig. 6 shows a noise-free image, noisy image and despeckling images by using different methods.

4. CONCLUSION

IVUS imaging is used to study the arterial wall structure, the evaluation of atherosclerotic diseases and diagnosis aspects. These medical images are generally corrupted by multiplicative speckle noise. The main objectives of this paper are, to give an overview about despeckling techniques in both spatial and transform domain, and also propose a new Shearlet shrinkage despeckling technique based on ACO. The proposed despeckling technique has been successfully applied to solve many combinatorial optimization problems (time-frequency domain). The results evaluation conclude that the Shearlet transform with three different type of threshold selection is faster and more efficient comparing to the other available techniques such as spatial filters or wavelet based methods. Shearlet transform based on ACO include various additional functionalities which make this method yields acceptable results. This method can obtain a favorable PSNR, and MSE) and successfully improve the quality of images and edges and curves as well according to CNR, and FOM.

REFERENCES

[1] C. Guy, and D. ffytche, "An Introduction to the principles of medical imaging," Revised edition, Imperial College Press, pp.267-294, 2005.

[2] M. Lorenz, W. Matthias, et al. "Prediction of clinical cardiovascular events with carotid intima-media thickness: a systematic review and meta-analysis," Circulation 115.4 :459-467, 2007.

[3] G. Garcìa, M. Hector, et al. "IVUS-based imaging modalities for tissue characterization: similarities and

differences," The international journal of cardiovascular imaging 27.2 (2011): 215-224.

[4] S. K. Narayanan and R. S. D. Wahidabanu, "A view on despekling in ultrasound imaging," International Journal of Signal Processing, Image Processing and Pattern Recognition, vol. 2, no. 3, pp. 85–98, September 2009.

[5] Yu, Yongjian, and Scott T. Acton. "Speckle reducing anisotropic diffusion," IEEE Transactions on image processing11.11 :1260-1270, 2002.

[6] O. Michailovich, A. Tannenbaum, "Despeckling of medical ultrasound images," IEEE transactions on ultrasonics, ferroelectrics, and frequency control 53.1 :64-78, 2006.

[7] N. S. Swamy, and E. Plotkin, "Despeckling of medical ultrasound images using data and rate adaptive lossy compression," IEEE Transactions on Medical Imaging 24.6 :743-754, 2005.

[8] R. C. Gonzalez and R. E. Woods, *Digital Image Processing*, Addison-Wesley Publishing Company, 2002.

[9] T. Loupas, W. N. Mcdicken, and P. L. Allen, "An adoptive weighted median filter speckle suppression in medical ultrasound images," IEEE Trans. Circuits Sys., vol. 36, pp. 129-135, 1989.

[10] A. K. Jain, Fundamentals of Digital Image Processing, 1st ed., Prentice – Hall, Inc, 1989.

[11] G. Pelin, A. Sertbas, and N. Ucan, "A wavelet-based mammographic image denoising and enhancement with homomorphic filtering." Journal of medical systems 34, no. 6 (2010): 993-1002.

[12] A. Alin, P. Tsakalides, and A. Bezerianos. "SAR image denoising via Bayesian wavelet shrinkage based on heavy-tailed modeling." IEEE Transactions on Geoscience and Remote Sensing 41, no. 8 (2003): 1773-1784.

[13] Zh. Ming, and K. Gunturk. "Multiresolution bilateral filtering for image denoising." IEEE Transactions on image processing 17.12 (2008): 2324-2333.

[14] R. Leonid, E. Fatemi. "Nonlinear total variation based noise removal algorithms." Physica D: nonlinear phenomena 60.1-4 (1992): 259-268.

[15] L. Rubio, and M. Nieves, "Kernel regression based feature extraction for 3D MR image denoising." Medical Image Analysis 15.4 (2011): 498-513.

[16] T. Tolga, "Principal components for non-local means image denoising." In Image Processing, 2008. ICIP 2008. 15th IEEE International Conference on, pp. 1728-1731. IEEE, 2008.

[17] J. Neumann and G. Steidl, "Dual-tree complex wavelet transform in the frequency domain and an application to signal classification," Int. J. Wavelets, Multiresolution and Inform. Process, vol. 3, no. 1, pp. 43-66, 2005.

[18] M. N. Do and M. Vetterli, "Contoulets: A directional multiresolution image representation," in Proc. IEEE Int. Conference on

Image Processing, New York, USA, Sep. 2002, pp. 357-360.

[19] E. J. Candes and D. L. Donoho, “Curvelets–A Surprisingly Effective Nonadaptive Representation for Object with Edges,” in Curve and Surface Fitting, A. Cohen, C. Rabut, and L. L. Schumaker, Ed. Saint-malo: Vanderbilt University Press, 1999.

[20] Lim, Wang-Q. "Nonseparable shearlet transform." IEEE transactions on image processing 22.5 (2013): 2056-2065.

[21] Sun, Hui, and Jia Zhao. "Shearlet threshold denoising method based on two sub-swarm exchange particle swarm optimization." In Granular Computing (GrC), 2010 IEEE International Conference on, pp. 449-452. IEEE, 2010.

[22] J. S. Lee, “Digital image enhancement and noise filtering by use of local statistics,” IEEE Trans. on Pattern Analysis and Machine Intelligence, vol. PAMI-2, no. 2, pp. 165-168, March 1980.

[23] N. Kingsbury, “Complex wavelets for shift invariant analysis and filtering of signals,” Appl. Comput. Harmon. Anal., vol. 10, no. 3, pp. 234-253, 2001.

[24] Dorigo, Marco, and Mauro Birattari. "Ant colony optimization." In Encyclopedia of machine learning, pp. 36-39. Springer, Boston, MA, 2011.

[25] Tian, Jing, Weiyu Yu, and Lihong Ma. "AntShrink: Ant colony optimization for image shrinkage." Pattern Recognition Letters 31.13 (2010): 1751-1758.

[26] A. Taki, et al. "Automatic segmentation of calcified plaques and vessel borders in IVUS images." International Journal of Computer Assisted Radiology and Surgery 3.3-4 (2008): 347-354.